Vietnam Journal of Science and Technology
DOI: https://doi.org/10.15625/2525-2518/22640

Optimization of SERS substrate performance by surface functionalization of glass in the photochemical method

Nguyen Thi Bich Ngoc[1,*], Nguyen Trong Nghia[1], Nguyen Thi Thuy[1], Nguyen Duc Toan[1], Doan Cat Cong[2], Pham Hong Minh[1], Nghiem Thi Ha Lien[1]

[1]*Institute of Physics, Vietnam Academy of Science and Technology, 18 Hoang Quoc Viet, Nghia Do Ward, Ha Noi, Viet Nam*
[2]*Graduate University of Science and Technology, Vietnam Academy of Science and Technology, 18 Hoang Quoc Viet, Nghia Do Ward, Ha Noi, Viet Nam*

[*]*Email: ntbngoc@iop.vast.vn*

Received: 1 April 2025; Accepted for publication: 18 August 2025

Abstract. Photochemical synthesis has gained popularity for the fabrication of high-performance surface-enhanced Raman scattering (SERS) substrates, eliminating the need for reagents or complex equipment. In this paper, a laser device system was designed and constructed using a pulsed laser diode with an emission wavelength of 405 nm. This system was employed to transform small spherical silver nanoparticles (AgNPs) into different morphological structures on glass substrates through the photochemical process. The morphology characteristics of AgNPs were controlled by the group functionalized on the glass surface, including hydroxyl (–OH), amin ($–NH_2$), and carboxyl (-COOH). The results obtained demonstrate that with $-NH_2$ group functionalized glass substrates ($G-NH_2$), the main product was the petal-shaped AgNPs after an irradiation time of 150 s. In addition, due to the presence of multiple $–NH_2$ functional groups, the number of AgNPs on the glass surfaces increased significantly and was distributed more evenly. The morphological characteristics of AgNPs on the $G-NH_2$ influence the performance of SERS substrates. By optimizing the morphology characteristics of AgNPs on glass through $–NH_2$ functional groups, the optimal SERS substrate provided an enhancement factor (EF) of 1.5×10^7 for melamine, with good uniformity and reproducibility, as indicated by a relative standard deviation (RSD) of 10.3 % and 4.7 %, respectively.

Keywords: photochemical synthesis, SERS substrates, silver nanoparticles, group functionalized glass surface, SERS.

Classification numbers: 2.1.1, 2.4.2.

1. INTRODUCTION

One of the most essential applications of AgNPs is SERS, a high-performance analytical tool. In SERS, the strong localized surface plasmon resonance (LSPR) of AgNPs enhanced the Raman signal of the analyte molecules. The fabrication method of SERS substrates is a key

factor in determining the magnitude of LSPR and the enhancement [1, 2]. Due to the development of nanotechnology and the ever-growing demand for SERS substrates, AgNPs can be fabricated through primary methods, including physical, chemical, and biological methods [3, 4]. By using chemical methods, silver ions are reduced to AgNPs in various solutions and materials. This method is the most popular because it is simple, convenient, and does not require expensive equipment. However, the synthesis process frequently uses reducing agents, stabilizing agents, and surfactants. These agents can affect the accuracy of the SERS measurement by hindering the adsorption of analytes onto the surfaces of AgNPs or interfering with SERS signals [5–9]. Fabricating AgNPs using physical methods often requires specialized, expensive equipment and extremely high temperatures and vacuum conditions [10–12]. Biological methods rely on numerous naturally derived materials and microorganisms, such as biomolecules, bacteria, plants, viruses, yeast, fungi, algae, and living cells and organisms, to fabricate AgNPs. Although this method has many advantages, such as easy availability, the use of non-toxic chemicals, environmental friendliness, and a simple synthesis method with low cost, it is not often used for SERS applications. Many organic chemical compounds and generating by-products can affect the SERS signal [4, 13].

The photochemical approach is gaining significant attention for synthesizing SERS substrates by using photons to directly or indirectly drive chemical reactions due to the restricted use of chemicals as reducing and stabilizing agents. By using photochemical synthesis, nanoparticles can be obtained in various media, ranging from solutions to solid materials. Moreover, among all fabrication methods for AgNPs used in SERS substrates, the photochemical approach offers several comparative advantages, including the use of simple and inexpensive equipment, versatility, controllable synthesis, and room-temperature operation [3, 13–15]. Research groups primarily focus on generating AgNP colloids and depositing them onto various substrates to create SERS substrates using photochemical techniques. For example, Condorelli's group used a laser to grow seed AgNPs into silver nanoplate colloids in the presence of H_2O_2 and applied Rhodamine 6G detection, with the EF obtained at approximately 10^4 [16]. Silver nanodecahedron colloids were also successfully synthesized by some research groups under light-emitting diode (LED) irradiation. The average EF using these particles is estimated to be in the order of 10^6 [17–19]. Other types of nanostructures, such as Tetrahedra or Pentagonal nanorods, were also fabricated using the photochemical method. The Zhou and Pietrobon research group reported that these particles produced highly sensitive SERS substrates with an EF of about 10^7 [20, 21].

The different research directions are the direct synthesis of AgNPs on various substrate materials using the photochemical method to generate SERS substrates. AgNP seeds were grown into grating-like nanostructures [22] or nanoplates [23] on the surface of silicon through a photochemical process using a femtosecond laser, with detection limits for Rhodamine of 10^{-7} M and 3 x 10^{-15} M, respectively. In addition to silicon, glass is also another typical substrate for photochemical fabrication of SERS substrates. AgNPs can be produced on glass surfaces [24, 25] to create SERS substrates or on more specialist glass surfaces, including optical fiber surfaces [26] or microfluidic channels [2]. All of these studies demonstrate the capacity to generate a variety of morphologies of AgNPs on glass surfaces, ranging from isotropic to anisotropic, by regulating the photoirradiation process. The obtained SERS substrates perform excellently in detecting substances at low concentrations. To produce flexible 3D SERS substrates, AgNPs were also photochemically synthesized on soft, porous materials, including paper [27, 28], chitosan films [29], graphene [30], and diatoms [31]. The photo-irradiation conditions, such as power, time, light, or chemical precursor, frequently modify the

characteristics of AgNPs formed directly on substrates using photochemical techniques without considering the substrate surface properties [2, 24, 25, 27].

Tailoring the physicochemical properties of substrates has emerged as a pivotal approach in the development of high-performance surface-enhanced Raman scattering (SERS) platforms. Specifically, modulation of surface chemistry, surface energy, and electrostatic interactions plays a crucial role in facilitating the controlled nucleation, stable adhesion, and uniform distribution of plasmonic metal nanoparticles. Numerous studies have demonstrated that chemically functionalized glass substrates enable effective immobilization of pre-synthesized noble metal nanoparticles, thereby significantly enhancing the sensitivity, reproducibility, and stability of SERS responses [32, 33]. For instance, functionalization of glass surfaces with amine ($–NH_2$) groups via (3-aminopropyl)triethoxysilane (APTES) treatment has been shown to promote electrostatic interactions with citrate-capped AgNPs, enabling their self-assembly into a densely packed and homogeneous monolayer. Such substrates exhibited excellent SERS performance, achieving detection limits down to 10^{-10} M for Rhodamine B and 10^{-8} M for Methylene Blue [32]. Moreover, to enhance the binding affinity for metallic nanostructures, thiol (–SH)-functionalized surfaces have also been employed, exploiting the strong chemisorption between thiol groups and metallic species such as Ag^0 and Au^0 [34, 35]. Another strategy involves the pre-functionalization of glass substrates with specific anchoring groups (e.g., –OH, $–NH_2$, –COOH, –SH) to increase their affinity toward silver ions (Ag^+) or pre-synthesized nanoparticle seeds, thereby facilitating localized nucleation and anisotropic growth during subsequent photochemical or chemical reduction processes [24, 36, 37].

In this work, we systematically investigate the influence of surface functional groups on the photochemical transformation and distribution of AgNPs on glass substrates. Pre-synthesized spherical AgNPs seeds were immobilized on glass surfaces functionalized with hydroxyl (–OH), amine ($–NH_2$), and carboxyl (–COOH) groups, followed by photochemical treatment using a 405 nm pulsed laser diode to form AgNPs. The morphology and distribution of AgNPs on glass substrates were found to influence the performance of the resulting SERS strongly substrates in detecting melamine.

2. MATERIALS AND METHODS

2.1. Materials

Reagents

Silver nitrate ($AgNO_3$), sodium hydroxide (NaOH), tri-natriumcitrat-dihydrat sodium citrate ($C_6H_5Na_3O_7.2H_2O$), 3-(Triethoxysilyl)-propylamine ($C_9H_{23}NO_3Si$, APTES), carboxyethylsilanetriol sodium salt ($C_3H_6O_5Na_2Si$), potassium hydroxide (KOH), melamine, ethanol were purchased from Sigma Aldrich. Glass substrates were obtained from China. The solution was prepared using DI water (resistance > 1 MΩ).

Instruments

AgNPs on glass substrates were prepared using a pulsed laser diode with an emission wavelength of 405 nm and a power of 12 mW (Roithner, Austria). The diameter of the focused laser image obtained from a glass surface was approximately 3.3 µm. A three-dimensional translation stage (PZ 2000FT, ASI, (x, y): 100 nm; z: 2 mm) was mounted in an optical microscope (TiE2, 10x).

2.2. Preparation of SERS substrates

The schematic diagram of the experimental setup to prepare the AgNPs on glass substrates with a pulsed laser diode is illustrated in Figure 1. First, AgNPs seeds solution was synthesized by the solution of citrate ($5x10^{-4}$ M), $AgNO_3$ ($5x10^{-4}$ M), NaOH ($5x10^{-3}$ M), and DI water under vigorous magnetic stirring. After the addition of NaOH, the solution immediately turned pale yellow.

Glass slides were cut to dimensions of 0.5 cm x 1.0 cm and washed with chromic acid and water. To prepare the OH group-functionalized surface (G-OH), glass slides were immersed in a 1 M KOH solution for 15 minutes. Afterward, the G-OH substrates were washed several times with water to remove excess from the surface. G-OH substrates were immersed in APTES 1 % and ethanol solution for 15 minutes to cover the glass surface with NH_2 groups (G-NH_2). To create carboxyl functional groups on the glass surface substrates (G-COOH), the G-OH substrates were submerged in a 1 % carboxyethylsilanetriol sodium salt solution in ethanol. The G-NH_2 and G-COOH substrates were washed three times with ethanol to remove excess chemicals.

Glass substrates with various functional groups on the surface, including glass, G-OH, G-NH_2, and G-COOH substrates, were immersed in a Petri dish containing 2 ml of AgNP seeds solution. The petri dish was then placed on the translation stage and irradiated by the pulsed laser diode at 405 nm with a power of 12 mW at room temperature for a duration of 150 s. Finally, these substrates were washed with DI water to remove the loosely bound ions and then dried at room condition. These SERS substrates were stored at 4 °C.

2.3. Melamine detection test of SERS substrates

Melamine was dissolved in water at various concentrations. A 5 µL melamine solution was deposited onto the glass substrates at the sites containing AgNPs and dried in air at room temperature before measuring the Raman spectra.

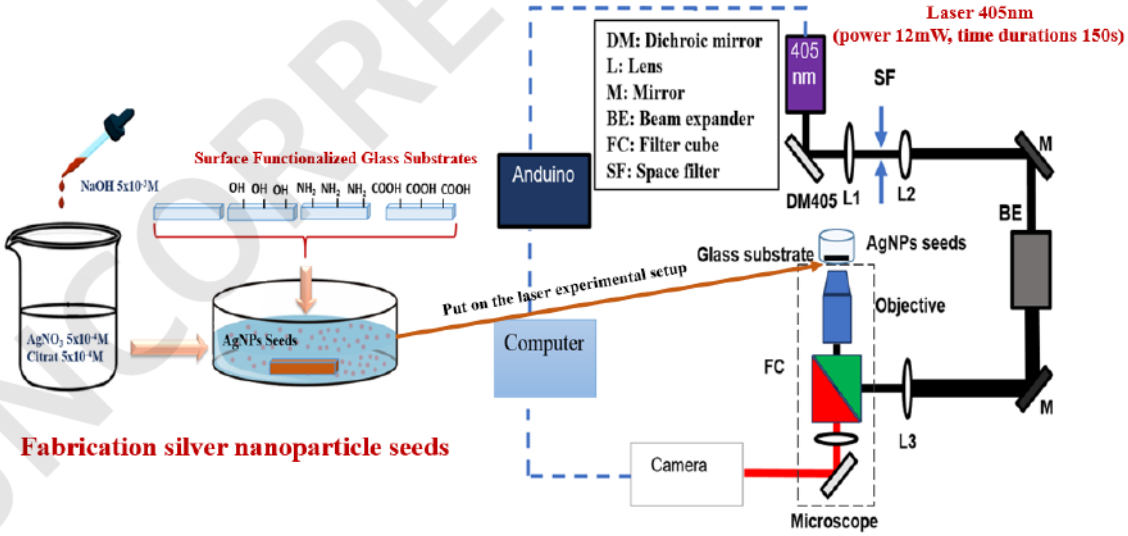

Figure 1. Schematic illustration of AgNPs fabrication on glass via laser experimental setup.

2.4. Characterization

The features of AgNP seeds were obtained by the Zeta potential measurement system (HORIBA SZ-100). The morphology of AgNPs on glass substrates was analyzed by FE-SEM (HITACHI Regulus 8100). The EDS measurements were recorded using a Hitachi Regulus 8100 Field Emission Scanning Electron Microscope. The SERS signal was obtained using a Raman spectroscope (Labram HR Evolution) with an excitation wavelength of 633 nm, an acquisition time of 10 seconds, and a laser spot size of 1 μm.

3. RESULTS AND DISCUSSION

Several research groups have elucidated the mechanism of the photochemical reaction that produces AgNPs in the presence of citrate [2, 14, 38]. In this case, citrate acts as both a photoreducing agent and controls the growth of the AgNP seeds in petal shape. Figure 2 shows a FESEM image and zeta potential of fabricated AgNP seeds. The average size of these spherically shaped AgNP seeds is around 20 nm and monodisperse.

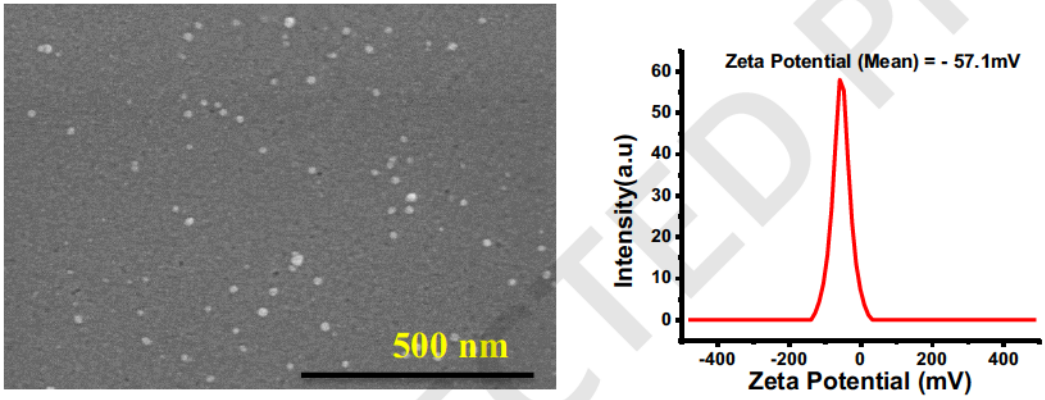

Figure 2. FESEM image and Zeta potential of AgNPs seeds.

The morphology characteristics of the AgNPs on glass substrates were tuned by changing the functional groups on the substrate's surface. Figure 3 shows FESEM images of AgNPs prepared on glass substrates with various functional groups under the same irradiation conditions: 12 mW power and 150 s of time. The growth of AgNPs on a glass substrate via the photocatalytic method is closely related to the presence of citrate, which is added to the solution during the stage of seed particle manufacturing and serves as a photo-reducing agent in addition to stabilizing the particles in solution [2, 14, 38], through the reaction:

$$\text{Citrate} + \lambda \rightarrow \text{Acetone-1,3-dicarboxylate} + CO_2 + 2e^- \quad (1)$$

$$Ag_n + e^- \rightarrow Ag_n^- \quad (2)$$

$$Ag_n^- + Ag^+ \rightarrow Ag_{n+1} \quad (3)$$

When a 405 nm laser illuminates the seed AgNPs solution, it induces the transformation of surface citrate, as shown in Eq. (1). The remaining two carboxyl groups bind to the surface of the seed AgNPs, transferring electrons to the seed nanoparticles and facilitating the reduction of excess Ag^+ ions in the solution onto the surface of the seed AgNPs through reactions (2) and (3). This process leads to the growth of larger AgNPs. Experimental studies have also shown

that no transformation occurs in the absence of citrate [2, 14, 38]. Unlike the synthesis of AgNPs in solution, the formation of AgNPs on glass substrates is significantly influenced by the interaction between the seed AgNPs and the substrate surface.

AgNPs are photochemically produced similarly on unfunctionalized glass substrates (Figure 3a) and G-OH (Figure 3b), with some AgNPs aggregating to form petals and spherical AgNPs with an average diameter of approximately 50 nm. However, the petals are more significant than the unfunctionalized glass substrates, and more AgNPs appear on the G-OH substrates. The growth of AgNPs on the glass substrate by photochemical reaction is based on the fact that more nanoparticles agglomerate. The photochemical reaction and agglomeration of seed silver nanoparticles (AgNPs) can occur both in solution and on the surface of glass substrates. These AgNP seeds tend to agglomerate together, forming larger spherical nanoparticles. When immobilized on the substrate surface and continued to be irradiated, they can further aggregate into petal-like nanostructures. Although non-functionalized glass substrates lack intentional surface modification, they inherently possess a small number of hydroxyl (–OH) groups on their surface. As a result, limited formation of flower-like AgNP structures can still be observed on these untreated substrates, albeit with lower density and uniformity compared to those with deliberate surface functionalization. On both kinds of substrates, though, the AgNPs are not evenly attached and do not cover the entire substrate surface. These morphology characteristics are related to the adsorption of AgNP seeds on the glass substrate surface by charge interaction. The charge interaction plays a vital role in the adsorption ability of AgNP seeds on the surface of glass substrates.

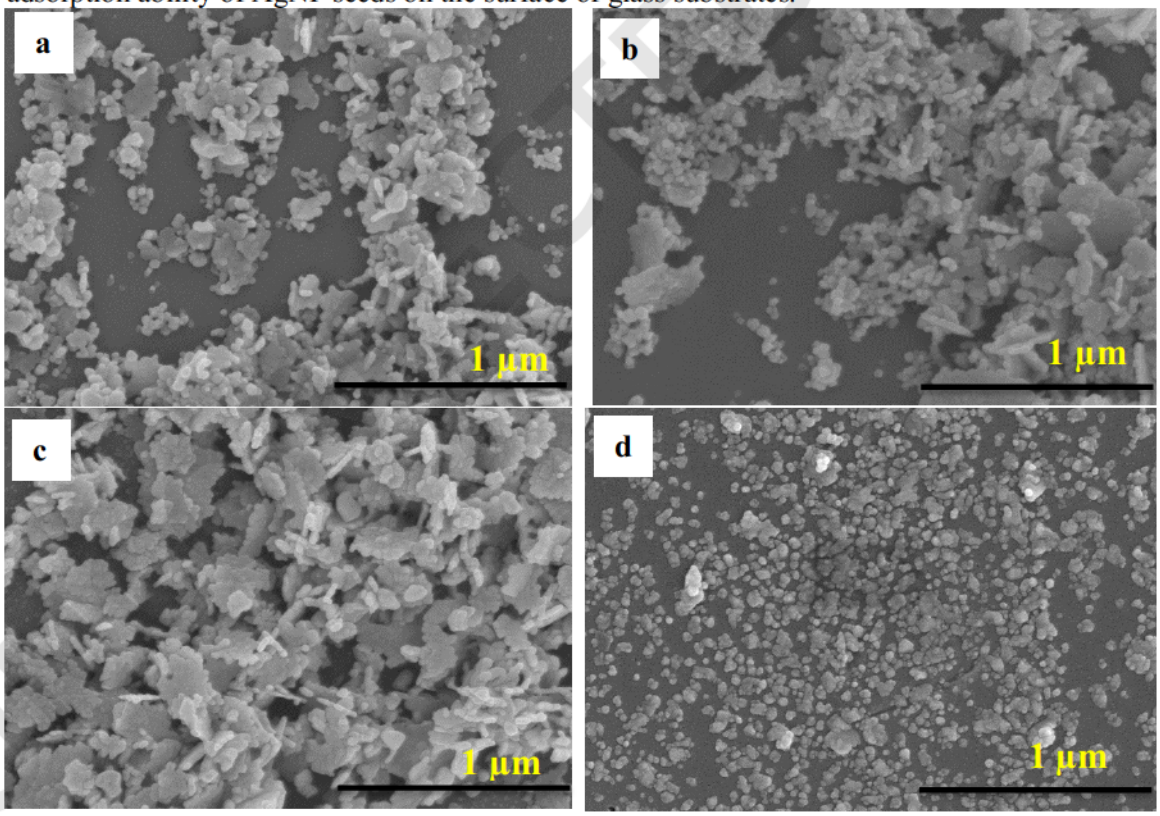

Figure 3. FESEM images of AgNPs on non-functionalized glass substrates (a), glass substrates with various functional groups on the surface, including G-OH (b), G-NH_2 (c), and G-COOH (d) substrates.

The surface charge of colloidal AgNP seeds was determined by a Zeta potential measurement system with an average zeta potential of -57mV (Figure 2). This Zeta potential indicated that the charge at the particle surface of AgNP seeds is a negative charge, which was attributed to the presence of sodium citrate on the particle surface. Therefore, the unfunctionalized glass surface and G-OH are covered with hydroxyl groups, resulting in a negatively charged surface that lacks the opportunity for electrostatic attraction of the AgNP seeds [24]. In contrast, for positively charged G-NH_2 substrates, AgNP seeds adhered abundantly and evenly to the glass substrate surface. The result is that the fabricated AgNPs mainly aggregate together to form petals, distributed relatively evenly and covering almost the entire surface of the substrate (Figure 3c). As a result, compared to other substrates fabricated under identical conditions, the amount of AgNPs produced and adhered to the G-NH_2 substrate's surface is significantly higher. Especially in the case of G-COOH substrates, the resulting morphology characteristics are quite different from those of other functional groups. The obtained AgNPs on G-COOH are clusters of two or three AgNPs sparsely clustered on the substrate surface (Figure 3d). The number of AgNPs adhering to the G-COOH substrates was also equally low. With a larger, negatively charged surface created by the carboxyl functional group, the strong repulsion between the two-like charges prevents the AgNPs produced during laser irradiation from forming much on the glass substrate surface. The formation of small AgNP clusters on the G-COOH substrate may be due to the growth from excess Ag^+ ions in the seed solution absorbed on the G-COOH surface by electrostatic attraction. The results obtained for the morphological properties of AgNPs on G-NH_2 substrates are comparable to those published by Zhen Yin's research group, which used non-functionalized glass substrates. However, to achieve such a morphological structure, they had to use 10 times the irradiation intensity and 10 times our irradiation time [2]. Therefore, the functionalization of the NH_2 functional group on the glass substrate surface has optimized the fabrication conditions.

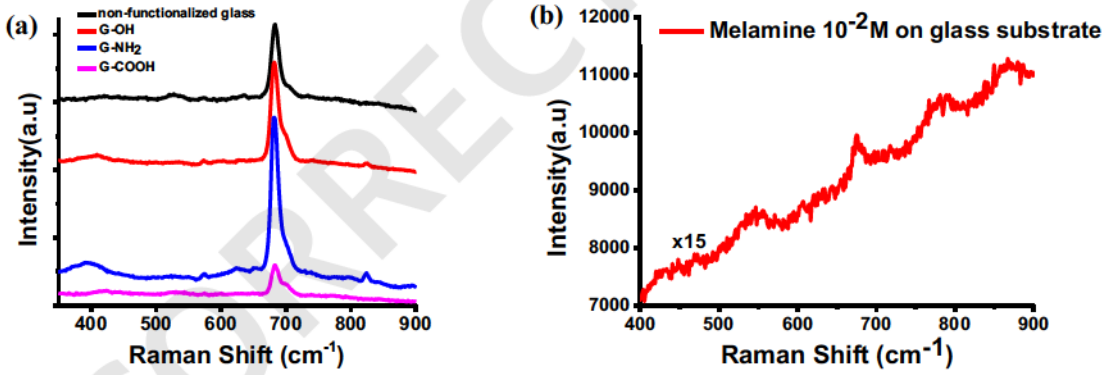

Figure 4. The SERS spectra of melamine 10^{-4}M on SERS substrates with various surface functional groups (a) and Raman spectra of melamine 10^{-2}M on glass (b).

To evaluate the SERS performance of SERS substrates, melamine at a concentration of 10^{-4} M was selected as the probe molecule. Figure 4a shows the SERS spectra of melamine collected from these SERS substrates using glass substrates with different surface functional groups. The characteristic peaks of melamine in the SERS spectra were located at 682 cm^{-1}, which corresponds to the ring breathing vibration in melamine molecules. In comparison to the intense peak at 674 cm^{-1} in the Raman spectrum of 10^{-2} M melamine on glass (Figure 4b), the characteristic peak of melamine on SERS substrates shifts to higher wavenumbers as a result of its interaction with the silver surface [33]. It can be observed that this peak appears on all SERS

substrates with various surface functional groups, though its intensity varies. The peak intensity at 682 cm^{-1} of the SERS substrates also clearly demonstrates that the substrate prepared with the G-NH_2 substrate exhibits the highest Raman enhancement, as shown in Figure 4a. The observed magnitude of the SERS signal can be explained by the surface morphologies of the AgNPs on glass substrates fabricated with various glass surface functional groups. From the SEM images of AgNPs on G-NH_2 (Figure 2c), a large number of petal AgNPs provide much more hot spots to concentrate the electromagnetic field, thus resulting in much stronger SERS performance. By comparison with the SERS substrates fabricated using non-functionalized glass (Figure 2a) and the G-OH substrates (Figure 2b), the AgNPs do not completely cover the substrate surface, resulting in a small number of AgNP petals and a limited number of formed hotspots. Therefore, the SERS performance of fabricated AgNPs on these two substrates is lower than on the G-NH_2 substrate. For the AgNPs on G-COOH substrates, the peak intensity is significantly lower than that of the other substrates. This is entirely consistent with the results obtained from the morphological characteristics of AgNPs, which are sparsely distributed on the G-COOH substrate, as observed in the SEM image in Figure 2d.

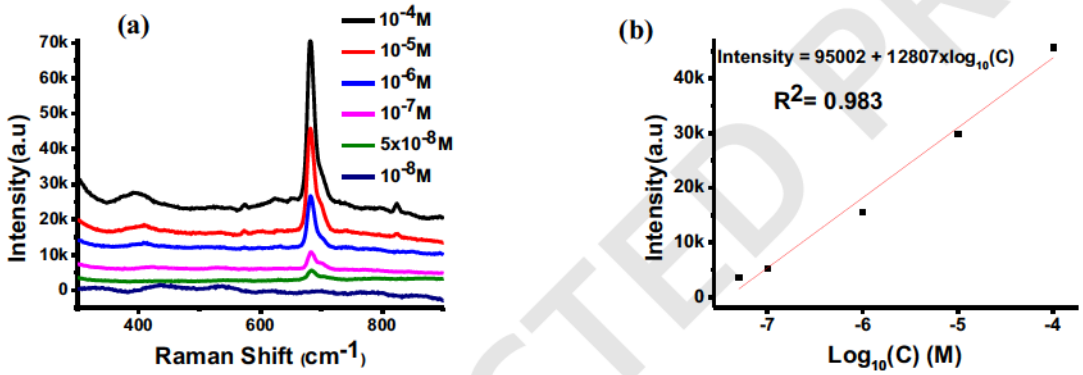

Figure 5. SERS spectra of melamine with different concentrations on the optimal SERS substrate (a). The peak intensity of melamine at 682 cm^{-1} as a function of various concentrations in log scale (b).

The SERS sensitivity of the optimal SERS substrates was evaluated by measuring SERS signals of melamine at different concentrations (10^{-4} – 10^{-8} M), as shown in Figure 5a. It can be observed that a low concentration of $5x10^{-8}$ M for melamine can be readily clearly identified, indicating that using the G-NH_2 substrate allows the production of SERS substrates have good SERS activity. In addition, a linear relationship was observed between the peak intensity at 682 cm^{-1} and the logarithmic concentration of melamine, with a high correlation coefficient (R^2 = 0.983) and the regression equation as: Intensity = 95002 + 12807xlog_{10}(C) (Figure 5b).

Because the Raman scattering spectra were measured under the same conditions, the magnitude of the EF to evaluate the detection efficiency of melamine is calculated according to the following equation:

$$EF = \left(\frac{I_{SERS}}{I_{Raman}}\right)\left(\frac{C_{Raman}}{C_{SERS}}\right)$$

where I_{SERS} and I_{Raman} represent the peak intensity of the SERS signal and the normal Raman signal obtained from AgNPs on G-NH_2 substrate as SERS-active substrate (Figure 5) and glass (Figure 7) as reference substrate, respectively. Here, the characteristic band at 682 cm^{-1} for melamine, along with the concentration of melamine on SERS substrates and glass substrates, was selected for calculation. Specifically, the concentrations were C_{SERS} = 10^{-7} M and C_{Raman} =

10^{-2} M. I_{SERS} and I_{Raman} were 5718 a.u. and 37 a.u., respectively. The EF is calculated to be 1.5 × 10^7, indicating a high SERS performance of SERS substrates fabricated using G-NH_2 substrates.

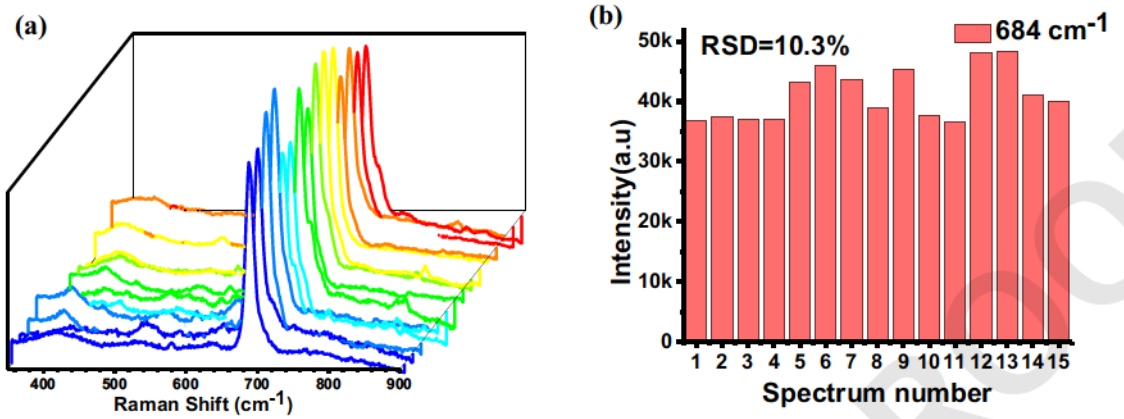

Figure 6. (a) SERS spectra and (b) intensity distribution at 684 cm^{-1} for 10^{-4}M melamine collected from 15 random sites on a SERS substrate.

To evaluate the signal uniformity of SERS substrates, the SERS spectra of melamine (10^{-4} M) at 15 random spots on the optimal substrate were collected, as depicted in Figure 6a. The relative standard deviation (RSD) was calculated following equation [39]:

$$SD = \sqrt{\frac{\sum_1^n (x_i - \bar{x})^2}{n-1}} \qquad RSD = \frac{SD}{\bar{x}} \times 100\ (\%) \tag{4}$$

where SD is the standard deviation, x_i denotes the Raman signal intensity at 682 cm^{-1} at the i-th time of melamine, and $\bar{x}$ implies the average Raman signal intensity, n = 15. The RSD values of optimal SERS substrates obtained in this experiment were approximately 10.3 %, confirming that this SERS substrate has good homogeneity.

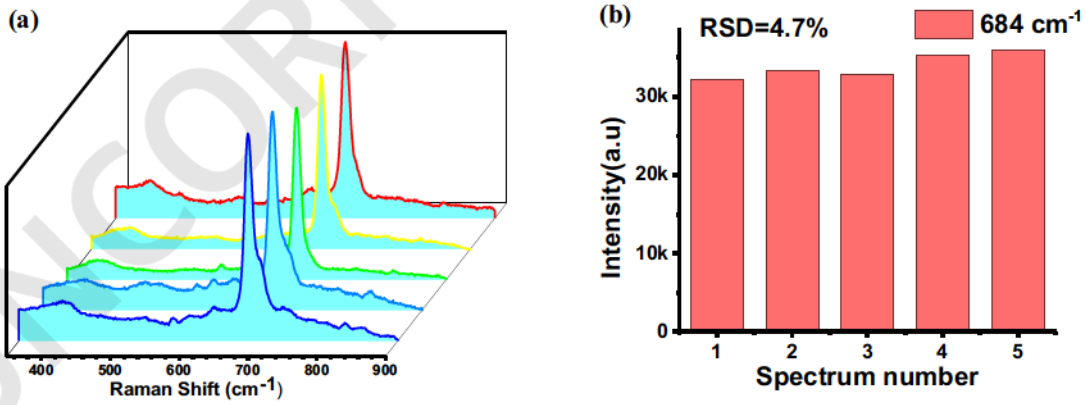

Figure 7. (a) SERS spectra and (b) intensity distribution at 682 cm^{-1} for 10^{-4}M melamine measured from 5 SERS substrates.

Moreover, the batch-to-batch reproducibility was evaluated by obtaining the SERS signals of melamine from 5 different SERS substrates, as shown in Figure 7a. The RSD value of the peak intensity at 682 cm^{-1} was calculated to be 4.7 % (Figure 7b). Good reproducibility of SERS substrates can be achieved by using G-NH_2 for photochemical fabrication method.

4. CONCLUSIONS

In summary, the SERS substrates were synthesized using a photochemical method with a pulsed laser diode emitting at 405 nm. The morphology characteristic of SERS substrates was optimized by modifying the surface functional group of glass substrates, including hydroxyl (-OH), amine (-NH_2), and carboxyl (-COOH) functional groups. Due to positively charged G-NH_2 substrates, the fabricated AgNPs mainly have petal shapes, are distributed relatively evenly, and cover almost the entire surface of the substrate. The optimal SERS substrate exhibited a high EF (1.5×10^7), good signal uniformity (RSD = 10.3 %), and superior batch-to-batch reproducibility (RSD = 4.7 %). These results indicate that fabricated SERS substrates using G-NH_2 substrates in the photochemical method have broad application potential for detecting low-concentration analytes.

Acknowledgments. This study was supported by the Vietnam Academy of Science and Technology (VAST) with grant number VAST01.02/25-26. We are also grateful for the use of the joint optics lab facilities between IOP and GUST, VAST.

CRediT authorship contribution statement. Nguyen Thi Bich Ngoc: Conceptualization, Methodology. Nguyen Thi Thuy: Investigation, Formal analysis. Nguyen Trong Nghia, Nguyen Duc Toan, Doan Cat Cong: Investigation, Software. Nghiem Thi Ha Lien: Formal analysis. Pham Hong Minh: Formal analysis.

Declaration of competing interest. The authors declare that they have no known competing financial interests or personal relationships that could have appeared to influence the work reported in this paper.

REFERENCES

1. Kurnoothala R., Muthukumar V S., Vishnubhatla K. C. – Facile fabrication of integrated microfluidic SERS substrate by femtosecond laser sintering of silver nano particles. Opt. Mater., **111** (2021) 110518. https://doi.org/10.1016/j.optmat.2020.110518.
2. Yin Z., He H., Wang Z., et al. – Facile in situ photochemical synthesis of silver nanoaggregates for surface-enhanced Raman scattering applications. Nanomaterials, **10** (2020) 685. https://doi.org/10.3390/nano10040685.
3. Lin S. K., Cheng W. T. – Fabrication and characterization of colloidal silver nanoparticle via photochemical synthesis. Mater. Lett., **261** (2020) 127077. https://doi.org/10.1016/j.matlet.2019.127077.
4. Koo S. – Flexible heater fabrication using amino acid-based ink and laser-direct writing. Micromachines, **13** (2022) 2209. https://doi.org/10.3390/mi13122209.
5. Lee S.-W., Chang S.-H., Lai Y.-S., et al. – Effect of temperature on the growth of silver nanoparticles using plasmon-mediated method under the irradiation of green LEDs. Materials, **7** (2014) 7781–7798. https://doi.org/10.3390/ma7127781.
6. Abbas R., Luo J., Qi X., et al. – Silver nanoparticles: Synthesis, structure, properties and applications. Nanomaterials, **14** (2024) 1425. https://doi.org/10.3390/nano14171425.
7. Fiévet F., Ammar-Merah S., Brayner R., et al. – The polyol process: A unique method for easy access to metal nanoparticles with tailored sizes, shapes and compositions. Chem. Soc. Rev., **47** (2018) 5187–5233. https://doi.org/10.1039/C7CS00777A.

8. Parashar M., Shukla V. K., Singh R. – Metal oxides nanoparticles via sol-gel method: A review on synthesis, characterization and applications. J. Mater. Sci. Mater. Electron., **31** (2020) 3729–3749. https://doi.org/10.1007/s10854-020-02994-8.
9. Yang G., Park S.-J. – Conventional and microwave hydrothermal synthesis and application of functional materials: A review. Materials, **12** (2019) 1177. https://doi.org/10.3390/ma12071177.
10. Gonzalez M. I. G., Bachmatiuk A., Bezugly V., et al. – Electron-beam induced synthesis of nanostructures: A review. Nanoscale, **8** (2016) 11340–11362. https://doi.org/10.1039/c6nr01941b.
11. Kim M., Osone S., Kim T., Higashi H., Seto T. – Synthesis of nanoparticles by laser ablation: A review. KONA Powder Part. J., **34** (2017) 80–90. https://doi.org/10.14356/kona.2017009.
12. Manawi Y. M., Ihsanullah, Samara A., Al-Ansari T., Atieh M. A. – A review of carbon nanomaterials' synthesis via the chemical vapor deposition (CVD) method. Materials, **11** (2018) 822. https://doi.org/10.3390/ma11050822.
13. Jara N., Milán N. S., Rahman A., et al. – Photochemical synthesis of gold and silver nanoparticles—A review. Molecules, **26** (2021) 4585. https://doi.org/10.3390/molecules26154585.
14. Pascu B., Negrea A., Ciopec M., et al. – Silver nanoparticle synthesis via photochemical reduction with sodium citrate. Int. J. Mol. Sci., **24** (2023) 255. https://doi.org/10.3390/ijms24010255.
15. Kazancioglu E. O., Aydin M., Arsu N. – Photochemical synthesis of nanocomposite thin films containing silver and gold nanoparticles with 2-thioxanthone thioacetic acid-dioxide and their role in photocatalytic degradation of methylene blue. Surf. Interfaces, **22** (2021) 100793. https://doi.org/10.1016/j.surfin.2020.100793.
16. Condorelli M., Scardaci V., D'Urso L., Puglisi O., Fazio E., Compagnini G. – Plasmon sensing and enhancement of laser prepared silver colloidal nanoplates. Appl. Surf. Sci., **475** (2019) 633–638. https://doi.org/10.1016/j.apsusc.2018.12.265.
17. Lu H., Zhang H., Yu X., Zeng S., Yong K.-T., Ho H.-P. – Seed-mediated plasmon-driven regrowth of silver nanodecahedrons (NDs). Plasmonics, **7** (2012) 167–173. https://doi.org/10.1007/s11468-011-9290-8.
18. Vu X. H., Dien N. D., Ha Pham T. T., et al. – The sensitive detection of methylene blue using silver nanodecahedra prepared through a photochemical route. RSC Adv., **10** (2020) 38974. https://doi.org/10.1039/D0RA07869G.
19. Tuan Anh M. N., Nguyen D. T. D., Ke Thanh N. V., Phuong Phong N. T., Nguyen D. H., Nguyen-Le M.-T. – Photochemical synthesis of silver nanodecahedrons under blue LED irradiation and their SERS activity. Processes, **8** (2020) 292. https://doi.org/10.3390/pr8030292.
20. Zhou J., An J., Tang B., et al. – Growth of tetrahedral silver nanocrystals in aqueous solution and their SERS enhancement. Langmuir, **24** (2008) 10407–10413. https://doi.org/10.1021/la800961j.
21. Pietrobon B., McEachran M., Kitaev V. – Synthesis of size-controlled faceted pentagonal silver nanorods with tunable plasmonic properties and self-assembly of these nanorods. ACS Nano, **3** (2009) 21–26. https://doi.org/10.1021/nn800591y.
22. Lin C.-H., Jiang L., Chai Y.-H., Xiao H., Chen S.-J., Tsai H.-L. – One-step fabrication of nanostructures by femtosecond laser for surface-enhanced Raman scattering. Opt. Express, **17** (2009) 21581–21589. https://doi.org/10.1364/oe.17.021581.
23. Ran P., Jiang L., Li X., Li B., Zuo P., Lu Y. – Femtosecond photon-mediated plasma enhances photosynthesis of plasmonic nanostructures and their SERS applications. Small, **15** (2019) 1804899. https://doi.org/10.1002/smll.201804899.
24. Lau D., Furman S. – Fabrication of nanoparticle micro-arrays patterned using direct write laser photoreduction. Appl. Surf. Sci., **255** (2008) 2159–2161. https://doi.org/10.1016/j.apsusc.2008.07.073.
25. Zaier M., Vidal L., Hajjar-Garreau S., Bubendorff J.-L., Balan L. – Tuning the morphology of silver nanostructures photochemically coated on glass substrates: An effective approach to large-scale functional surfaces. Nanotechnology, **28** (2016) 105603. https://doi.org/10.1088/1361-6528/28/10/105603.
26. Pham T. B., Hoang T. H. C., Pham V. H., et al. – Detection of permethrin pesticide using silver nano-dendrites SERS on optical fibre fabricated by laser-assisted photochemical method. Sci. Rep., **9** (2019) 12590. https://doi.org/10.1038/s41598-019-49077-1.

27. Rajapandiyan P., Yang J. – Photochemical method for decoration of silver nanoparticles on filter paper substrate for SERS application. J. Raman Spectrosc., **45** (2014) 574–580. https://doi.org/10.1002/jrs.4502.
28. Assylbekova G., Alotaibi H. F., Yegemberdiyeva S., et al. – Sunlight induced synthesis of silver nanoparticles on cellulose for the preparation of antimicrobial textiles. J. Photochem. Photobiol., **11** (2022) 100134. https://doi.org/10.1016/j.jpap.2022.100134.
29. Gabriel J. S., Gonzaga V. A. M., Poli A. L., Schmitt C. C. – Photochemical synthesis of silver nanoparticles on chitosans/montmorillonite nanocomposite films and antibacterial activity. Carbohydr. Polym., **171** (2017) 202–210. https://doi.org/10.1016/j.carbpol.2017.05.021.
30. Nguyen T. L., Do T. C., Ngo X. D., et al. – Photochemical decoration of silver nanoparticles on graphene oxide nanosheets and their optical characterization. J. Alloys Compd., **615** (2014) 843–848. https://doi.org/10.1016/j.jallcom.2014.07.042.
31. León-Valencia A., Briceño S., Reinoso C., et al. – Photochemical reduction of silver nanoparticles on diatoms. Mar. Drugs, **21** (2023) 185. https://doi.org/10.3390/md21030185.
32. Truc Phuong N. T., Dang V. Q., Van Hieu L., et al. – Functionalized silver nanoparticles for SERS amplification with enhanced reproducibility and for ultrasensitive optical fiber sensing in environmental and biochemical assays. RSC Adv., **12** (2022) 31352–31362. https://doi.org/10.1039/D2RA06074D.
33. Tran N. L. N., Tho L. H., Tran N. Q., et al. – Integrating the amino-functionalized MOF-5 film with the silver nanoparticle substrate for a high SERS enhancement effect and long-term stability. Mater. Adv., **5** (2024) 4401–4408. https://doi.org/10.1039/d4ma00087k.
34. Mosier-Boss P. – Review of SERS substrates for chemical sensing. Nanomaterials, **7** (2017) 142. https://doi.org/10.3390/nano7060142.
35. Ilie C.-I., Spoială A., Motelica L., et al. – Ag NP-decorated glass surfaces for sensing in medical applications. Coatings, **15** (2025) 426. https://doi.org/10.3390/coatings15040426.
36. Do Quynh Nhu N., Nguyen T.-A., Tran Truc Phuong N., et al. – Facile fabrication of SERS substrates by the electrodeposition method to detect pesticides with high enhancement effect and long-term stability. Langmuir, **40** (2024) 13292–13302. https://doi.org/10.1021/acs.langmuir.4c01651.
37. D'Agostino A., Taglietti A., Grisoli P., et al. – Seed mediated growth of silver nanoplates on glass: Exploiting the bimodal antibacterial effect by near IR photo-thermal action and Ag^+ release. RSC Adv., **6** (2016) 70414–70423. https://doi.org/10.1039/c6ra11608f.
38. Scardaci V. – Anisotropic silver nanomaterials by photochemical reactions: Synthesis and applications. Nanomaterials, **11** (2021) 2226. https://doi.org/10.3390/nano11092226.
39. Nguyen N. T. B., Nguyen T. T., Nguyen N. T., et al. – Multi-shape silver nanoparticles on filter paper by the chemical reduction method. J. Nanopart. Res., **25** (2023) 126. https://doi.org/10.1007/s11051-023-05777-4.